University of Massachusetts - Amherst
ScholarWorks@UMass Amherst

Physics Department Faculty Publication Series | Physics

2003

K ->pi pi electroweak penguins in the chiral limit

V Cirigliano

JF Donoghue
University of Massachusetts - Amherst, donoghue@physics.umass.edu

Eugene Golowich
University of Massachusetts - Amherst, golowich@physics.umass.edu

K Maltman

Follow this and additional works at: http://scholarworks.umass.edu/physics_faculty_pubs

Part of the Physics Commons

Cirigliano, V; Donoghue, JF; Golowich, Eugene; and Maltman, K, "K ->pi pi electroweak penguins in the chiral limit" (2003). *Physics Department Faculty Publication Series.* Paper 103.
http://scholarworks.umass.edu/physics_faculty_pubs/103

This Article is brought to you for free and open access by the Physics at ScholarWorks@UMass Amherst. It has been accepted for inclusion in Physics Department Faculty Publication Series by an authorized administrator of ScholarWorks@UMass Amherst. For more information, please contact scholarworks@library.umass.edu.

arXiv:hep-ph/0209332v1 27 Sep 2002

$K \to \pi\pi$ Electroweak Penguins in the Chiral Limit

V. Cirigliano [a*] , J.F. Donoghue and E. Golowich [b †], K. Maltman [c ‡]

[a]Departament de Física Teòrica, IFIC, Universitat de València - CSIC ,
Apt. Correus 22085, E-46071 València, Spain

[b]Physics Department, University of Massachusetts,
Amherst MA 01003 USA

[c]Dept. of Mathematics and Statistics, York University, 4700 Keele St., Toronto ON M3J 1P3 Canada,
and CSSM, University of Adelaide, Adelaide 5005, SA, Australia

We report on dispersive and finite energy sum rule analyses of the electroweak penguin matrix elements $\langle(\pi\pi)_2|\mathcal{Q}_{7,8}|K^0\rangle$ in the chiral limit. We accomplish the correct perturbative matching (scale and scheme dependence) at NLO in α_s, and we describe two different strategies for numerical evaluation.

1. Introduction

The subject of this talk is the calculation of the $K \to \pi\pi$ matrix elements of the electroweak penguin operators, conventionally denoted as $\mathcal{Q}_7$ and $\mathcal{Q}_8$ [1]. Interest in these quantities is twofold. First, the Standard Model prediction of ϵ'/ϵ depends crucially on the K-to-2π matrix elements of the QCD penguin ($\mathcal{Q}_6$) and EW penguin ($\mathcal{Q}_8$) operators, [1,2,3]:

$$\frac{\epsilon'}{\epsilon} = 20{\cdot}10^{-4}\left[-2.0{\cdot}\frac{\langle\mathcal{Q}_6\rangle_0}{\mathrm{GeV}^3}\,(1-\Omega_{\mathrm{IB}})-0.50{\cdot}\frac{\langle\mathcal{Q}_8\rangle_2}{\mathrm{GeV}^3}\right],$$

where the above matrix elements are evaluated in the $\overline{MS}$-NDR renormalization scheme at scale $\mu = 2$ GeV. Secondly, the leading term in the chiral expansion of $\langle\mathcal{Q}_{7,8}\rangle$ can be related to the $V-A$ QCD correlator with flavor ud, whose spectral function is experimentally accessible through τ decays [4,5]. This provides the opportunity to perform a data-driven evaluation of hadronic matrix elements, whose results can then be confronted with other non-perturbative techniques (like Lattice QCD and $1/N_c$ expansion). Therefore electroweak penguins provide an interesting theoretical laboratory for kaon physics.

2. Summary of formal results

Our first goal is to relate the $K \to \pi\pi$ matrix elements to the observable spectral functions. The first large step is done for us by chiral symmetry, which relates $\langle\pi\pi|\mathcal{Q}_{7,8}|K\rangle$ to vacuum expectation values of two 4-quark operators [6]

$$\begin{aligned}\langle(\pi\pi)_2|\mathcal{Q}_7|K^0\rangle_{p^0} &= -\frac{2}{F_0^3}\,\langle\mathcal{O}_1\rangle\ ,\\ \langle(\pi\pi)_2|\mathcal{Q}_8|K^0\rangle_{p^0} &= -\frac{2}{F_0^3}\,\left[\frac{1}{3}\langle\mathcal{O}_1\rangle+\frac{1}{2}\langle\mathcal{O}_8\rangle\right],\end{aligned}$$

where F_0 is the pion decay constant in the chiral limit and the definitions of O_1 and O_8 can be found in Ref. [6]. The above relations receive NLO chiral corrections (whose order of magnitude is $\sim m_K^2/(4\pi F_\pi)^2 = 0.18$) which have been investigated within chiral perturbation theory [7].

The second step consists in relating the v.e.v.'s of $O_{1,8}$ to the $V-A$ QCD correlator $\Delta\Pi_{ud}(s) \equiv \Pi_{\mathrm{V}}^{(0+1)}(s) - \Pi_{\mathrm{A}}^{(0+1)}(s)$, with flavor structure ud [4]. The outcome is that:

- $\langle O_1\rangle$ is related to the integral of $s^2\Delta\Pi(s)$ over all spacelike momenta;

*Speaker at QCD02. Research supported in part by EC-Contract ERBFMRX-CT980169, by MCYT, Spain (Grant No. FPA-2001-3031), and by ERDF funds from the European Commission

†Research supported in part by the NSF under Grant PHY-9801875

‡Research supported in part by the Natural Science and Engineering Research Council of Canada

[4]For details on the notation we refer to Ref. [8]

- $\langle O_8 \rangle$ is related to the leading singularity of $\Delta\Pi(s)$ at short distance (large spacelike momenta).

Essential tools in a formal derivation of the above results and in relating $\langle O_{1,8} \rangle$ to the spectral function are the dispersive representation of the correlator

$$\Delta\Pi(Q^2) = -\frac{2F_\pi^2}{m_\pi^2 + Q^2} + \int_{s_{\rm thr}}^{\infty} ds \, \frac{\Delta\rho(s)}{s + Q^2} \, . \qquad (1)$$

and the operator product expansion (OPE) representation, valid for large space-like momenta $Q^2 \gg \Lambda_{\rm QCD}^2$, which, through $\mathcal{O}(\alpha_s^2)$, has the form

$$\Delta\Pi_{OPE}(Q^2) \sim \sum_{d \geq 2} \frac{1}{Q^d} \left[a_d(\mu) + b_d(\mu) \ln \frac{Q^2}{\mu^2} \right] . \qquad (2)$$

$a_d(\mu)$ and $b_d(\mu)$ are combinations of vacuum expectation values of local operators of dimension d. In the chiral limit, the above sum begins with a_6, whose NLO expression is [5]:

$$a_6(\mu) = (2\pi\alpha_s + A_8 \alpha_s^2) \langle O_8 \rangle + A_1 \alpha_s^2 \langle O_1 \rangle \, . \qquad (3)$$

The formal analysis is summarized by

$$\begin{pmatrix} \langle O_1 \rangle_\mu \\ \langle O_8 \rangle_\mu \end{pmatrix} = \hat{M}(\alpha_s) \begin{pmatrix} I_1(\mu) + H_1(\mu) \\ I_8(\mu) - H_8(\mu) \end{pmatrix} \, , \qquad (4)$$

where the matrix $\hat{M}(\alpha_s)$ contains the matching coefficients at NLO in α_s, and encodes the correct renormalization scheme dependence. Its explicit form can be found in Refs. [8]. $I_{1,8}$ are related to the spectral function as follows,

$$I_1(\mu) = \int_0^\infty ds \; s^2 \ln \left(\frac{s + \mu^2}{s} \right) \Delta\rho(s) \qquad (5)$$

$$I_8(\mu) = \int_0^\infty ds \; \frac{s^2 \mu^2}{s + \mu^2} \; \Delta\rho(s) \qquad (6)$$

while $H_{1,8}$ are related to subleading (higher dimensional) terms in the short distance expansion:

$$H_1(\mu) = \sum_{d \geq 8} \frac{2}{d-6} \cdot \frac{a_d(\mu)}{\mu^{d-6}} \, , \qquad (7)$$

$$H_8(\mu) = \sum_{d \geq 8} \frac{a_d(\mu)}{\mu^{d-6}} \, . \qquad (8)$$

[5] The coefficients $A_{1,8}$ depend on the definition used for γ_5 in $d \neq 4$. They can be found in Ref. [8].

A close look at the input needed in Eq. (4) and at the database on $\Delta\rho$ (Refs. [4,5]) shows that data alone do not provide enough information for a reliable determination of the spectral integrals. In fact, we run out of data at $s = m_\tau^2$, while the weighs entering $I_{1,8}$ are growing with s. We therefore need to supply some extra theoretical input to optimize the use of data in this problem. Along this path, we have followed two approaches, which can be schematically characterized as follows:

I. Use of data plus QCD integral constraints (classical chiral sum rules). [8]

II. Use of data plus QCD duality (Finite Energy Sum Rules, FESR). [9]

3. Numerics I: Residual Weight Method

This approach is an efficient way to enforce the constraints from classical chiral sum rules [10,11] in the evaluation of the spectral integrals $I_{1,8}(\mu)$, which have the generic form:

$$I(\mu) = \int_0^\infty ds \, K(s,\mu) \, \Delta\rho(s) \, . \qquad (9)$$

The basic idea is to write $K(s,\mu)$ as the sum of an arbitrary combination of the weights $1, s$, and $s \log s$ and a residual term r, as follows:

$$K(s,\mu) = x \, 1 + y \, s + z \, s \log s + r_{(x,y,z)}(s,\mu) \, . \qquad (10)$$

From Eq. (10) and the chiral constraints one then has

$$I(\mu) = F_0^2 (x - z \frac{4\pi\delta M_\pi^2}{3\alpha}) + \int_0^\infty ds \, r(s,\mu) \, \Delta\rho(s), \qquad (11)$$

and can choose (x, y, z) (so far arbitrary) in such a way as to minimize the total uncertainty (associated with both the theoretical input for F_0 and δM_π^2, and the large errors on $\Delta\rho(s)$ for $s > 2.5$ GeV^2). The method is effective in those situations where choices for x, y, z exist which make $r \sim 0$ in the region with no data (but before the onset of asymptotia) without amplifying the effect of imprecise knowledge of F_0 and δM_π^2. Procedural details and intermediate results can be found in Ref. [8]. Here let us recall that the method leads to a reasonably accurate determination $I_{1,8}$ at different values of μ between 2 and

4 GeV (with accuracy deteriorating at large μ). This method tells us very little about the subleading terms $H_{1,8}$, which can be neglected only for sufficiently large μ. We have assumed that $H_{1,8}(\mu = 4\text{GeV}) = 0$ in Eq. (4) and used the NLO renormalization group equations to evolve the results down to the lower scale $\mu = 2$ GeV. Numerical results are reported in Sect. 5

4. Numerics II: FESR

In principle, this method allows us to determine the coefficients a_d appearing in the OPE expansion for the correlator $\Delta\Pi(s)$ in the asymptotic Euclidean region (Eq. (2)). The determination of a_6, in particular, provides a direct extraction of $\langle O_8 \rangle$ at $\mu = 2$ GeV. The determination of the a_d, $d \geq 8$, also allows one to estimate the combinations $H_{1,8}(\mu = 2\,\text{GeV})$, needed as input to the lower scale version of the RWM analysis, Eq. (4). Let us now summarize our implementation of the FESR analysis [9].

An FESR analysis, applied to a generic correlator $\Pi(s)$ with spectral function $\rho(s)$ is based on the following relation (consequence of Cauchy's theorem, and the analytic structure of the correlator):

$$J[w, s_0] + R[w, s_0] = f_w[s_0, \{a_d\}] \ . \tag{12}$$

Eq. (12) involves the spectral integral

$$J[w, s_0] = \int_{s_{th}}^{s_0} ds \ w(s)\rho(s) \ , \tag{13}$$

the integrated OPE (function of the various condensates)

$$f_w[s_0, \{a_d\}] = -\frac{1}{2\pi i} \oint_{|s|=s_0} ds \ w(s)\Pi_{\text{OPE}}(s) \ , \tag{14}$$

and the remainder term (arising from the difference $\Pi(s) - \Pi_{OPE}(s)$ on the $|s| = s_0$ circle)

$$R[w, s_0] = -\frac{1}{2\pi i} \oint_{|s|=s_0} ds \ w(s) \left(\Pi_{\text{OPE}} - \Pi\right) . \tag{15}$$

Eq. (12) is valid for any value of s_0 and any polynomial weight. However, the presence of $R[s_0, w]$ pollutes the extraction of the OPE coefficients a_d in terms of data through Eq. (12). Therefore it is highly desirable to work with a range of s_0 values and with weights $w(s)$ such that $R[w, s_0] << J[w, s_0]$. To accomplish this, we rely on the observation that for $|s|$ large enough ($s_0 \gg \Lambda^2_{QCD}$), the OPE provides a good representation of the full correlator along the whole circle, except in a region localized around the time-like axis. The physics of this breakdown is given by the arguments of Poggio, Quinn and Weinberg [12]. As a consequence one expects that weights with a zero at $s = s_0$, de-emphasizing the region where the OPE fails, are good candidates to generate a small-sized $R[w, s_0]/J[w, s_0]$ [6]. We use this as the basic guiding principle in the selection of weights for our analysis. The weights were also chosen to avoid large cancellations in the spectral integrals, which would lead to a poor statistical signal.

The lowest degree weights satisfying our criteria have degree 3. Two useful cases (with $y = s/s_0$) are:

$$w_1(y) = (1-y)^2 (1-3y) \tag{16}$$

$$w_2(y) = (1-y)^2 \, y \tag{17}$$

These choices imply that $f_{w_{1,2}}[s_0, \{a_d\}]$ depend on the dimension six and eight condensates, thereby allowing us to extract information on a_6 and a_8 from a least-square fit. The window of s_0 values used in the fit procedure is $1.95\,\text{GeV}^2 < s_0 < 3.15\,\text{GeV}^2$. The lower endpoint has been determined by trying ever lower values of s_0 until the extracted a_6 ceases to be consistent with the values obtained by the smaller analysis windows. From the ALEPH data we obtain (at $\mu = 2$ GeV):

$$a_6 = (-4.45 \pm 0.7) \cdot 10^{-3} \ \text{GeV}^6 \tag{18}$$

$$a_8 = (-6.2 \pm 3.2) \cdot 10^{-3} \ \text{GeV}^8 \tag{19}$$

with a correlation coefficient $c(a_6, a_8) = -0.99$. Although no precise answer emerges for a_8, we see that a_6 (directly related to $\mathcal{Q}_8$) can be determined fairly well. The errors reported above are essentially of statistical nature. In order to address potential systematic effects due to $R[s_0, w] \neq 0$ (duality violation), we have repeated the fit procedure using non-overlapping s_0 subwindows. We find that the fitted parameters in

[6] Supporting evidence for this fact has been found in Ref. [13], within an analysis of the V and A correlators.

the different analyses are consistent, thereby confirming that the effect of $R[s_0, w]$ is suppressed in this case. A more explicit portrait of the FESR machinery is obtained by plotting $J[w_{1,2}, s_0]$ and $f_{w_{1,2}}[s_0; a_6, a_8]$ as a function of s_0, as in Figs. 1,2. The excellent match of the OPE curve versus data increases our confidence that in this analysis duality violation is under control.

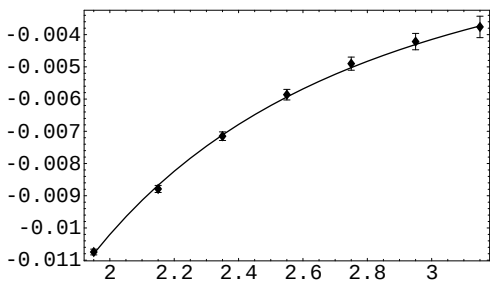

Figure 1. $f_{w_1}[s_0, a_6, a_8]$ (continuous curve) and $J[w_1, s_0]$ (data points) versus s_0 (GeV^2).

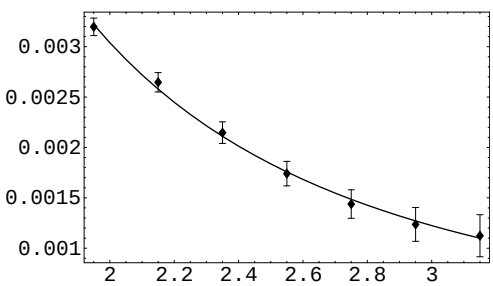

Figure 2. $f_{w_2}[s_0, a_6, a_8]$ (continuous curve) and $J[w_2, s_0]$ (data points) versus s_0 (GeV^2).

5. Results for $\langle(\pi\pi)_{I=2}|\mathcal{Q}_{7,8}|K^0\rangle$

Having outlined the two numerical strategies in the above sections, in Table 1 we report $\langle\mathcal{Q}_{7,8}\rangle$ in the $\overline{MS}$-NDR renormalization scheme at scale $\mu = 2$ GeV, from methods I, II, and VSA [7].

Procedures I and II lead to consistent results, with II having reduced uncertainty. The underlying reason is that method II exploits best the low-error part of experimental data. Both our results seem to point to moderate violation of VSA. For a comparison with other recent determinations [14,15,16,17,18] see Refs. [14,9]. Implications of our results for the value of ϵ'/ϵ in the Standard Model will be discussed in [9].

[7] The number reported corresponds to $(m_s+m_d)(2GeV) =$ 110 MeV.

Table 1
$\overline{MS}$-NDR results at $\mu = 2$ GeV and $n_f = 4$.

Method	$\langle\mathcal{Q}_7\rangle_{I=2}$/GeV^3	$\langle\mathcal{Q}_8\rangle_{I=2}$/GeV^3
I	0.16 ± 0.10	2.22 ± 0.70
II (ALEPH)	0.23 ± 0.05	1.41 ± 0.27
II (OPAL)	0.21 ± 0.05	1.72 ± 0.32
VSA	0.32	0.94

REFERENCES

[1] A. J. Buras, hep-ph/9806471.
[2] S. Bertolini, hep-ph/0206095.
[3] M. Ciuchini et. al, hep-ph/9503277.
[4] ALEPH Coll., R. Barate et al., Eur. Phys. J. C **4** (1998) 409.
[5] OPAL Coll., K. Ackerstaff et al., Eur. Phys. J. C **7** (1999) 571.
[6] J. F. Donoghue and E. Golowich, Phys. Lett. B **478** (2000) 172.
[7] V. Cirigliano and E. Golowich, Phys. Lett. B **475** (2000) 351, Phys. Rev. D **65** (2002) 054014.
[8] V. Cirigliano et al., Phys. Lett. **B 522** (2001) 245.
[9] V. Cirigliano, J.F. Donoghue, E. Golowich and K. Maltman, in preparation.
[10] S. Weinberg, Phys. Rev. Lett. **18** (1967) 507.
[11] T. Das et al., Phys. Rev. Lett. **18** (1967) 759.
[12] E. Poggio et al., Phys. Rev. D **13** (1976) 1958.
[13] K. Maltman, Phys. Lett. **B 440** (1998) 367.
[14] J. Bijnens et al., JHEP **0110**, (2001) 009 ; and hep-ph/0209089.
[15] M. Knecht et al., Phys. Lett. B **508** (2001) 117.
[16] S. Narison, Nucl. Phys. B **593** (2001) 3.
[17] E. Pallante et al., Nucl. Phys. B **617** (2001) 441.
[18] A. Donini et al., Phys. Lett. B **470** (1999) 233 ; CP-PACS Coll., J.-I. Noaki et al., hep-lat/0108013 ; RBC Coll., T. Blum et al., hep-lat/0110075 ; SPQ$_{CD}$R Coll., D. Becirevic et al., hep-lat/0209136.